

Interfacially active particles in droplet/matrix blends of model immiscible homopolymers: Particles can increase or decrease drop size

Prachi Thareja · Kevin Moritz · Sachin S. Velankar

Received: 16 April 2009 / Accepted: 14 December 2009 / Published online: 12 January 2010
© Springer-Verlag 2009

Abstract Particles have been shown to adsorb at the interface between immiscible homopolymer melts and to affect the morphology of blends of those homopolymers. We examined the effect of such interfacially active particles on the morphology of droplet/matrix blends of model immiscible homopolymers. Experiments were conducted on blends of polydimethylsiloxane and 1,4-polyisoprene blended in either a 20:80 or 80:20 weight ratio. The effects of three different particle types, fluoropolymer particles, iron particles, and iron oxyhydroxide particles, all at a loading of 0.5 vol.%, were examined by rheology and by direct flow visualization. Particles were found to significantly affect the strain recovery behavior of polymer blends, increasing or decreasing the ultimate recovery, slowing down or accelerating the recovery kinetics, and changing the dependence of these parameters on the applied stress prior to cessation of shear. These rheological observations were found to correlate reasonably well with particle-induced changes in drop size. The particles can both increase as well as decrease the drop size, depending on the particle type, as well as on which phase is continuous. The cases in which particles cause a decrease in drop size are analogous to the particle stabilization of “Pickering emulsions” well-known from the literature on oil/water systems. We hypothesize that cases in which particles increase drop size are analogous to the “bridging–dewetting” mechanism known in the aqueous foam literature.

Keywords Polymer blends · Pickering emulsions · Strain recovery · Interfacial tension · Compatibilizers

Introduction

Compatibilizers, conventionally block copolymers, are commonly used during the blending of immiscible homopolymers (Datta and Lohse 1996). The compatibilizer generally adsorbs at the interface between the immiscible phases and improves blending. In this paper, we are only concerned with blends that have a droplet/matrix morphology, and in this context, we define “improved blending” as a “decrease in mean drop size after any particular blending operation.” Such a decrease in drop size is believed to result from the ability of the compatibilizer to promote flow-induced breakup of drops as well as its ability to prevent their recoalescence during blending (Macosko et al. 1996; Milner and Xi 1996; Van Puyvelde et al. 2001).

This paper is concerned with “particulate compatibilizers”—particles that adsorb at the interface between the two immiscible homopolymers in a blend and can sometimes have effects that are similar to conventional block copolymer compatibilizers. This area of research has been stimulated by similar research in oil/water systems. In oil/water systems, it is well-recognized that particles that are partially wetted by oil and water can adsorb at the oil/water interface. Such particles can prevent coalescence of oil drops in water (or vice versa) and hence stabilize emulsions of oil and water. Such particle-stabilized emulsions are called Pickering emulsions (Binks 2002; Binks and Horozov 2006). This paper considers polymeric analogs of Pickering emulsions, viz., droplet/matrix

P. Thareja · K. Moritz · S. S. Velankar (✉)
Department of Chemical Engineering, University
of Pittsburgh, Pittsburgh, PA 15261, USA
e-mail: velankar@pitt.edu

blends of immiscible homopolymers with particles at the interface. There have been several investigations of particles (carbon black (Gubbels et al. 1994; Sumita et al. 1991; Zaikin et al. 2007), nanoclays (Hong et al. 2006; Ray et al. 2004; Si et al. 2006), silica (Elias et al. 2007, 2008; Vermant et al. 2004), etc.) adsorbed at the interfaces in polymer blends, and their effects on the morphology and properties of those blends. The preceding list of references is far from comprehensive, and a recent review article (Fenouillot et al. 2009) provides an excellent overview—and comprehensive citations—of this research. In some cases, particles can significantly improve blending (i.e., realize a finer-scale morphology) and hence the term “particulate compatibilizers.”

We are presently considering the effects of interfacially adsorbed particles in an immiscible blend system composed of polyisoprene (PI) and polydimethylsiloxane (PDMS). This blend is a “model” system in the sense that the two immiscible polymers are chosen for their experimentally convenient attributes, such as thermal stability, low cost, transparency, etc. Most importantly, both the polymers are viscous liquids at room temperature, and hence, the blends can be prepared by hand-mixing with a spatula, without requiring polymer processing equipment. Such model systems have already yielded much insight into the role of interfacial phenomena in uncompatibilized and compatibilized immiscible blends. Here, we seek to exploit these model blends to elucidate the role of interfacially active particles.

In a recent article, we showed that a wide variety of particle types readily adsorb at the interface between PDMS and PI (Thareja and Velankar 2008b). The present paper is focused on the specific question of whether those same particles can improve blending in droplet/matrix blends of PDMS and PI. If a decrease in drop size with added particles can be demonstrated—and especially if particles can be shown to suppress coalescence—then the particles may be regarded as good compatibilizers, and this system may be useful to elucidate the mechanisms whereby particles act as compatibilizers.

The principal experimental technique used in this paper is rheology. In droplet/matrix blends, much re-

search has revealed a close relationship between the mean drop size and the rheological properties of the blend (Tucker and Moldenaers 2002). For example, the timescale of the rheological transients (e.g., stress relaxation or strain recovery) scale with the mean drop size (Vinckier et al. 1999; Wang and Velankar 2006a). Accordingly, *trends* in drop size can be followed easily and accurately by following rheological transients rather than by direct imaging of the morphology. In particular, in this paper, we will infer changes in drop size from the strain recovery upon cessation of steady shear.

Experimental

Materials Some physical properties of the PI and PDMS homopolymers are listed in Table 1. These polymers were chosen as they were molten at room temperature, thus allowing flow experiments to be conducted at room temperature. Three different particle types listed in Table 2 were used in this research. SEM images of these particles are shown in Fig. 1. These same particle types were verified to be interfacially active at the PI/PDMS interface in our earlier research (Thareja and Velankar 2008b).

Blend preparation Particle-free blends were first prepared by blending the PI and the PDMS, either in an 80:20 weight ratio or in a 20:80 weight ratio. Blending was conducted by hand with a spatula. Once macroscopically homogeneous blends were prepared, particles were placed in a fresh Petri dish, the appropriate amount of blend was poured on the particles, and blending was continued until particles were well-dispersed in the blend. All blends presented in this article contained 0.5 vol.% of the particles. At this low loading, the particles did not affect the rheology of the bulk phases significantly. All samples were degassed under vacuum to remove the air bubbles before any rheology or visualization experiments were performed.

Blends are designated S_x - y where x is the weight fraction of the PDMS ($x = 20$ or 80), and y is the particle type. The two particle free blends are designated

Table 1 Homopolymers and their properties

Polymer	Supplier	MW (g/mol)	Viscosity (Pa s) ^a	Density ^b (kg/m ³)	Surface tension (mN/m)
Polydimethylsiloxane (PDMS)	Rhodia	135,600	96	960	19.2
Polyisoprene (PI)	Kuraray America	29,000	131	910	35.9

^aTerminal (i.e., low frequency plateau) complex viscosity $|\eta^*|$ at 25°C measured with an AR 2000 rheometer

^bQuoted by manufacturer

Table 2 Particle characteristics

Particles	Shape, average size (μm)	Density (g/cm^3)	Surface energy ^a (mN/m)	Supplier
PTFE	Irregular, 8	2.2	25–28.5	Dyneon
Iron oxyhydroxide (FeOOH)	Elongated, 0.6×0.1	4.03	63.3–72.3	Elementis pigments
Iron (Fe)	Spherical, 3	7.8	Uncertain; 46 for pure iron	ISP technology

^aSurface energy estimated by a “float-sink” method in (Thareja and Velankar 2008b)

S20-0 (for the blend with 20% PDMS) and S80-0 (for the blend with 80% PDMS).

Rheology Rheological experiments were conducted in stress controlled mode using an AR 2000 rheometer

with a cone-and-plate geometry (40 mm diameter, 1° cone). Sample temperature was maintained at 25°C using a Peltier plate. Samples were subjected to the shear history shown in Fig. 2. Samples were first sheared at 400 Pa for 2,000 strain units, then the subsequent strain recovery upon cessation of shear was monitored, followed by an oscillatory frequency sweep at 20% strain. This sequence (shear for 2,000 strain units, recovery, and oscillatory) was repeated at four successively lower stresses of 400, 200, 100, and 50 Pa. The results of the dynamic oscillatory measurements are not discussed in this paper but are published elsewhere (Thareja 2008). A limited number of repeat tests on samples showed reproducibility of ultimate strain to better than 0.02 strain units.

Visualization Samples were visualized in a home-built shear cell, which consists of two parallel glass plates. The bottom plate can be rotated at a controlled speed, driven by an ARES rheometer motor. The stationary top plate was fixed to the frame of the rheometer. The optical assembly consisted of a $\times 20$ microscope objective connected to a nose piece, and some additional optics feeding the image to a computer-controlled camera. The optics are mounted on a slide allowing any portion of the rotating geometry to be visualized. In this research, all visualization was conducted on a portion of sample at a distance of 10 mm from the center of rotation. It must be noted that, whereas the rheology experiments are stress-controlled, the visualization apparatus is based on an ARES motor, which makes it a strain controlled flow.

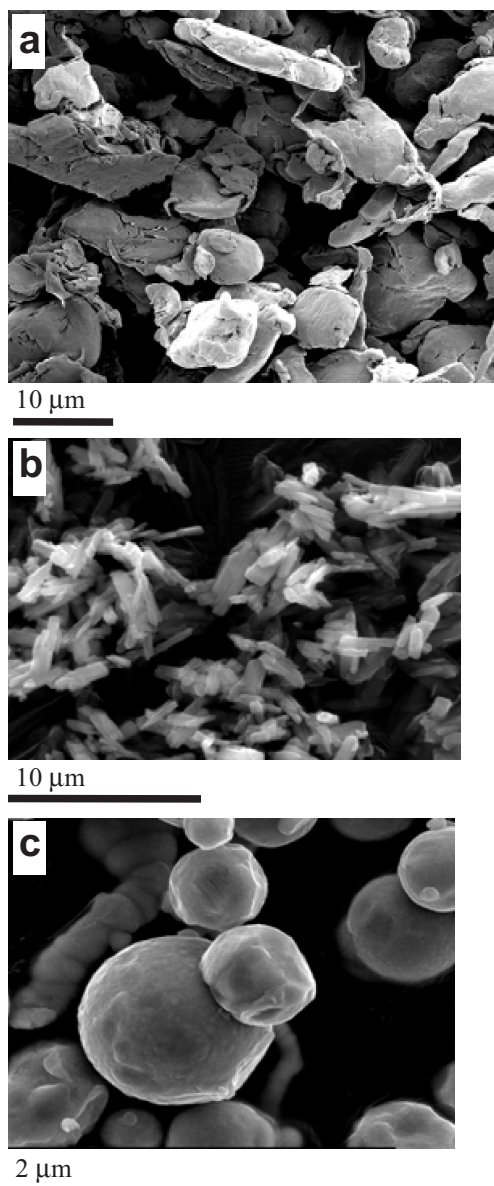


Fig. 1 SEM images of particles used in this research: **a** PTFE; **b** iron oxyhydroxide; **c** iron

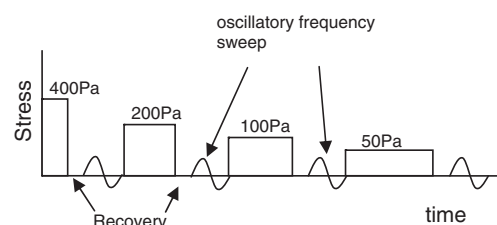


Fig. 2 Shear history applied to the blends. Each shearing step was 2,000 strain units, whereas each recovery was 5 min. Dynamic oscillatory measurements were conducted after each recovery but are not discussed in this paper

Theory: strain recovery and relationship to blend morphology

As mentioned in “[Introduction](#),” past research shows that rheological properties can serve as a convenient probe of morphological evolution in droplet/matrix blends. Much of the past research has focused on using small-amplitude dynamic oscillatory experiments for this purpose. Most commonly, the G' vs frequency data show a distinct relaxation that corresponds to shape relaxation of droplets (Graebling et al. 1993; Kitade et al. 1997; Vinckier et al. 1996). The timescale of this relaxation has been used successfully as a quantitative indicator of drop size.

However, the situation can be more complex when considering blends containing interfacially active particles. When drop surfaces are covered with particles, drops can adhere to each other, either due to attractions between the particles adsorbed on adjacent drops or due to particles simultaneously adsorbing on two drops (i.e. bridging; Ashby et al. 2004; Horozov and Binks 2006; Stancik and Fuller 2004). Accordingly, interfacially adsorbed particles can cause drops to adhere to each other and can induce gel-like behavior as evidenced by a low-frequency plateau in the G' vs frequency data (Thareja and Velankar 2007, 2008a). Indeed many of the blends studied here showed such weak gel-like behavior (Thareja 2008). Finally, the distribution of the particles in the two phases may also complicate the interpretation of the oscillatory data (Elias et al. 2007). This makes quantitative analysis of oscillatory data more complex. Instead, we will focus on an alternate rheological measurement: strain recovery. Certainly, the presence of interfacially active particles can complicate the mechanisms of strain recovery as well, and this is discussed in more detail at the end of this section. However, the advantage of strain recovery is that the data are readily amenable to quantitative analysis, in particular, the ultimate recovery can be obtained directly, and an average recovery time can be obtained by a simple data-fitting. Thus, the effects of the various particle types can be compared more readily.

The key methodology of this paper is the use of strain recovery after cessation of steady shear to track the evolution of the blend morphology. Here, we will first review the basic aspects of strain recovery in droplet/matrix blends in the absence of any interfacially active species.

Consider a droplet/matrix blend of mean drop radius R , drop volume fraction ϕ , drop viscosity η_d and matrix viscosity η_m , subjected to shear flow at a stress σ . The interfacial tension between the drop and the matrix

fluids is taken to be α , and the viscosity ratio $\frac{\eta_d}{\eta_m}$ is designated as p . During flow, the drops will deform and orient in the direction of flow, with the deformation being determined by the capillary number:

$$Ca = \frac{R\eta_m\dot{\gamma}}{\alpha} \quad (1)$$

If the flow is stopped, the drop retracts back into a spherical shape due to interfacial tension. Such drop retraction induces creep recovery (Vinckier et al. 1999). In this paper, the bulk phases are nearly Newtonian, and hence, almost all the recovery is attributable to the interfacial tension-driven drop retraction. However, in systems in which the bulk phases have significant viscoelasticity, there may be additional contributions to the creep recovery.

A linear viscoelastic model of blend rheology has been used previously to predict the dependence of the interfacial tension-driven recovery on the drop size (Vinckier et al. 1999). It has been shown that the creep recovery of a blend can be well-described by a single-exponential process:

$$\gamma = \gamma_\infty \left[1 - \exp\left(-\frac{t}{\lambda_{F2}}\right) \right] \quad (2)$$

where, γ_∞ is the ultimate recovery, and λ_{F2} is the time constant characterizing the recovery. Dimensional analysis suggests that

$$\gamma_\infty = \frac{R\sigma}{\alpha} f(\phi, p) \quad (3)$$

$$\lambda_{F2} = \frac{R\eta_m}{\alpha} g(\phi, p) \quad (4)$$

Expressions for the functions $f(\phi, p)$ and $g(\phi, p)$ have been discussed in previous publications (Vinckier et al. 1999; Wang and Velankar 2006a) but are not important here. In this paper, we are only concerned with the proportionality of γ_∞ and λ_{F2} on the drop size R suggested by Eqs. 3 and 4. Specifically, by monitoring changes in γ_∞ and λ_{F2} during any applied shear history, we can infer changes in the mean drop size during that shear history.

In the shear history used in this paper, the blends are subjected to a sequence of decreasing shear stresses (Fig. 2). We can consider two limiting cases:

Case I: Coalescence does not occur Lowering the stress usually causes an increase in drop size due to flow-induced coalescence. One of the goals of this paper is to test whether these particles, which were shown to be interfacially active in our previous work, also suppress coalescence. If flow-induced coalescence

does not occur upon reducing stress, R is independent of σ and that will be indicated by $\gamma_\infty \propto \sigma$ and λ_{F2} being independent of stress.

Case II: $Ca = Ca_{cr}$ If a blend is sheared for a sufficiently long time, the drops grow sufficiently large that their critical capillary number exceeds that for breakup. A steady-state balance between coalescence and breakup is then reached, and in this case, the capillary number is nearly equal to the critical capillary number for breakup Ca_{cr} . If this condition is realized in the shear history of Fig. 2, then the drop size R varies inversely with the stress, i.e., drop coalescence “exactly compensates” for a decrease in stress. In this case, γ_∞ is independent of stress, whereas $\lambda_{F2} \propto \sigma^{-1}$.

Certainly, behavior between these limits is also possible, where flow-induced coalescence does occur upon reducing stress, but R increases less slowly than σ^{-1} .

Past experiments on particle-free blends with a shear history similar to Fig. 2 reported behavior similar to, but not exactly, that predicted by Case II: specifically, γ_∞ decreased slightly with decreasing stress, whereas $\lambda_{F2} \propto \sigma^{-0.6}$ was observed (Martin 2007; Martin and Velankar 2007; Vinckier et al. 1999). This was interpreted as R increasing less steeply than σ^{-1} , although it must be reiterated that the above discussion is based on linear viscoelasticity, whereas the drop retraction-induced recovery may no longer be described by a linear viscoelastic rheological model under experimental conditions.

In contrast, Case I is difficult to observe experimentally in compatibilizer-free blends due to the difficulty of preventing coalescence or breakup upon changing shear stress. Nevertheless, Vinckier et al. (1999) were able to approximate conditions under which stress was changed, but drop size remained constant, and in that case, $\gamma_\infty \propto \sigma$ and λ_{F2} independent of stress was indeed observed (Vinckier et al. 1999).

Finally, we note that the entire discussion above strictly applies only to the particle-free blends S20-0 and S80-0. The presence of interfacially active particles may affect the creep recovery in several ways. Firstly, the particles may reduce the interfacial tension between the polymers and hence cause some of the same rheological effects noted with interfacially active compatibilizers. Specifically, compatibilizers can increase γ_∞ as well as slow down the recovery (Wang and Velankar 2006b), and particles that reduce interfacial tension may show the same effect. Secondly, if the particles are sufficiently crowded at the interface, they may immobilize the interface. This may be expected to reduce drop deformation and hence ultimate recovery. In the extreme case, crowded drops may not retract into

spherical shapes at all (Cheng and Velankar 2009), thus sharply reducing γ_∞ . Finally, particle-induced bridging may create a loose network of drops (Thareja and Velankar 2007, 2008a); the recovery of this network may produce a new mechanism for creep recovery. In summary, the creep recovery of particle-containing blends may be more complex than of particle-free blends. The broad trends that γ_∞ and λ_{F2} both increase with drop size are still expected to hold, and hence, changes in morphology can still be deduced from rheological experiments. Yet, it is important to verify all deductions about morphological changes by direct visualization.

Results

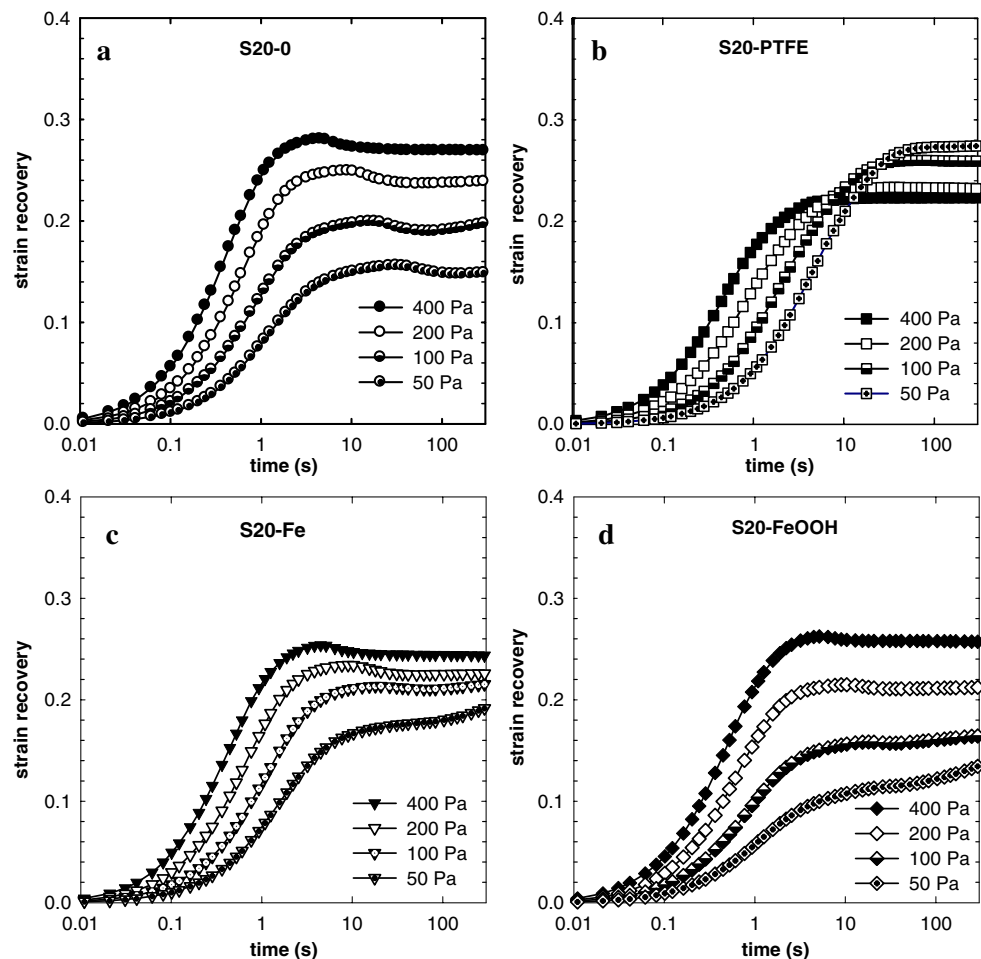
Rheology

Figures 3 and 4 show the strain recovery of all the blends and its dependence on stress. In this graph, and all subsequent graphs, the small amount of recovery due to the viscoelasticity of the bulk phases has been subtracted as a linear weighted average of the components as described previously (Wang and Velankar 2006a). Accordingly, the plotted data represent the recovery attributable to the interfacial tension driven retraction of drops. In no case was this subtracted bulk contribution more than 10% of the total recovery and, in most cases, was well under 5% of the total recovery.

Considering first the two particle-free blends S20-0 (Fig. 3a) and S80-0 (Fig. 4a), the recovery vs time data show that the ultimate recovery is typically a few 10% and is completed within a few seconds at all stress levels. The trends in γ_∞ and λ_{F2} will be considered quantitatively later, but it is immediately apparent that γ_∞ decreases with decreasing stress, whereas the kinetics of recovery slow down; that is, the recovery time increases. The later trend is consistent with flow-induced coalescence. In most cases, the recovered strain vs time curve shows an overshoot followed by a slight reversal of recovery, e.g., clearly evident in S80-0 after 400 Pa shearing. Such reversal of recovery has been noted previously in blends (Gramespacher and Meissner 1995; Wang and Velankar 2006a), but a mechanistic explanation has yet to be provided.

All six of the particle-containing blends show qualitatively the same trend in recovery kinetics: in all cases, decreasing stress slows down the recovery kinetics. In four of the particle-containing blends, S20-Fe and S20-FeOOH and S80-PTFE and S80-FeOOH, γ_∞ decreases with decreasing stress, similar to the particle-free blends. In contrast, in two blends, S20-

Fig. 3 Recovered strain vs time for **a** S20-0, **b** S20-PTFE, **c** S20-Fe, **d** S20-FeOOH. Every tenth point is shown



PTFE and S80-Fe, γ_∞ increases with decreasing stress, a trend that, to our knowledge, has never previously been seen in any rheological study of immiscible blends.

Based on a qualitative inspection of the data alone, it appears that, in all of the particle-containing blends, the recovery kinetics always slow down when the stress reduces; that is, none of the blends show a complete suppression of coalescence. Certainly, that does not imply that particles do not affect drop size, and this will be examined further; yet, it is important to emphasize that the ability to prevent coalescence, which is generally considered to be an important characteristic of good compatibilizers, is not observed with any of these particles.

To more clearly gauge the effect of particles, we undertake a more quantitative analysis of the trends in γ_∞ and the recovery kinetics with decreasing stress. γ_∞ can be obtained directly from the data of Figs. 3 and 4. As expected from previous research, the data for the two particle-free blends can be well-fitted by Eq. 2 (as an example, see the lowest curve in Fig. 5). Accordingly, the single-exponential time λ_{F2} resulting from these fits completely characterizes the recovery kinetics of

these two blends. For the six particle-containing blends, Eq. 2 does not always give good fits (see upper two curves in Fig. 5). In this case, the fitting parameter λ_{F2} characterizes the recovery kinetics only approximately.

γ_∞ and λ_{F2} thus obtained for all the blends are plotted as a function of stress in Figs. 6 and 7. These data can be postulated to have a power law dependence on stress, and the corresponding power law exponents are listed in Table 3. Note that range of stresses covered is less than an order of magnitude, and furthermore, the bulk contribution subtracted from the total recovery does affect the power law exponents somewhat, especially for the S80 samples. Hence, the power law exponents cannot ascribe any fundamental significance and are only to be regarded as a convenient way to compare the various samples.

The two particle-free blends S20-0 and S80-0 show similar trends. In both cases, γ_∞ is weakly dependent on stress (exponents of 0.28 and 0.19), whereas λ_{F2} increases as stress decreases with exponents close to -0.6 as also noted previously (Martin 2007). These trends indicate that the trend in drop size is intermediate between the two cases discussed in the previous section

Fig. 4 Recovered strain vs time for **a** S80-0, **b** S80-PTFE, **c** S80-Fe, **d** S80-FeOOH. Every tenth point is shown

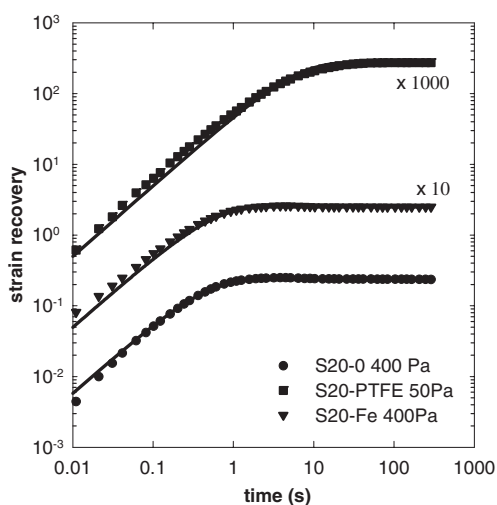
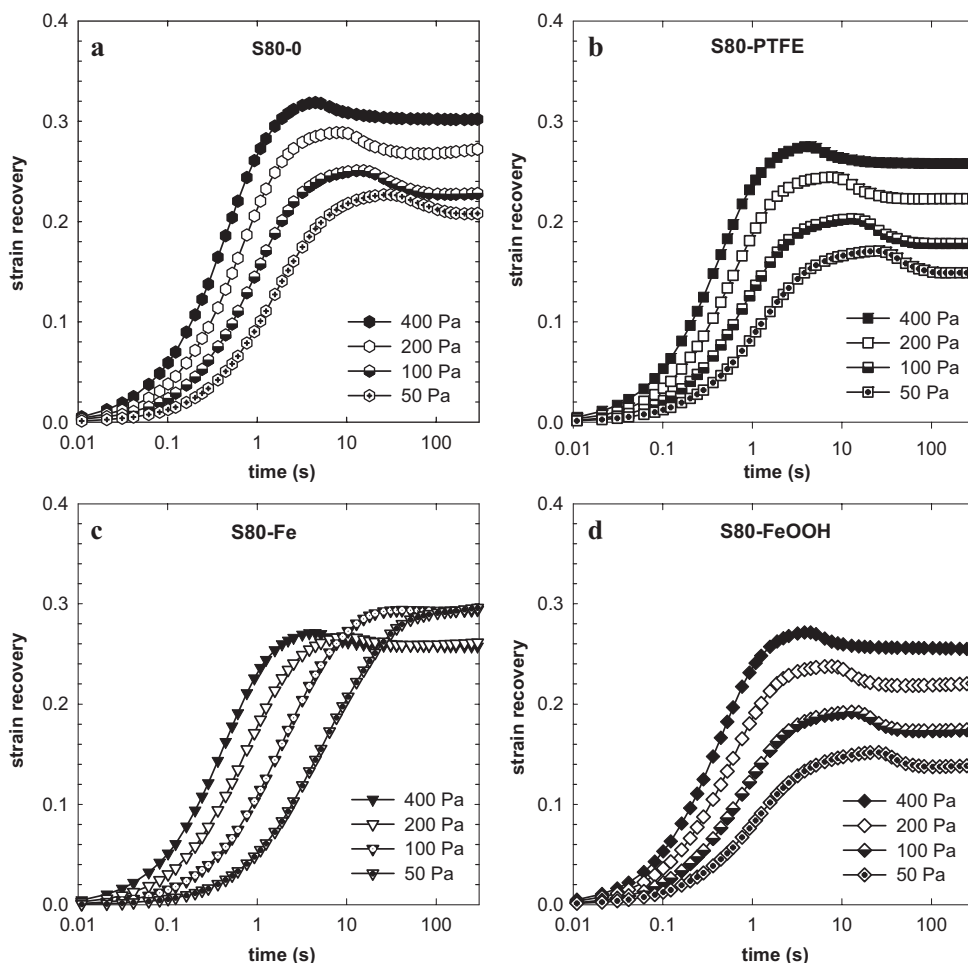


Fig. 5 Sample fits to single exponential recovery kinetics (Eq. 2) for three blends after shearing at the stress levels specified in the caption. Note that the recovery curves have been shifted up by the factors noted in the graph for clarity

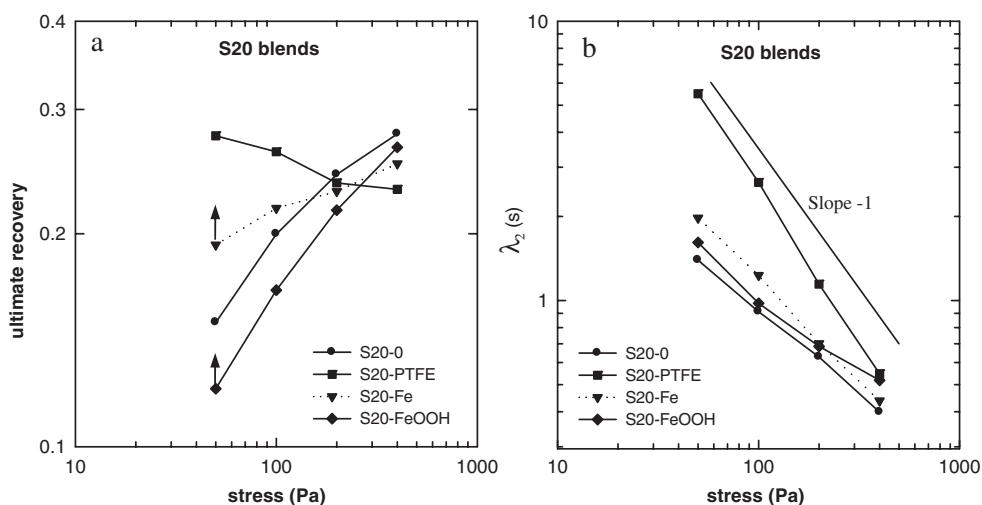
entitled “Theory: strain recovery and relationship to blend morphology”: Decreasing shear stress does permit coalescence; however, the increase in drop size R is less sharp than σ^{-1} , and hence, the capillary number decreases upon shearing at the lower stress levels.

Comparing the behavior of the particle-containing blends with the corresponding particle-free ones, three kinds of behavior may be distinguished:

S20-FeOOH, S80-FeOOH, and S80-PTFE For these three blends, the trends in γ_{∞} and λ_{F2} with decreasing stress are quite similar to that for the corresponding particle-free blends, and the exponents are similar in magnitude. Quantitatively, however, the γ_{∞} and λ_{F2} of these particle-containing blends are significantly smaller than of the corresponding particle-free blends, possibly indicating that particles reduce the absolute value of the drop size. We will examine this point below by direct visualization.

S20-PTFE and S80-Fe For both these blends, a qualitative inspection of the data showed that γ_{∞} increases

Fig. 6 Variation of **a** γ_∞ and **b** λ_{F2} with stress for S20 blends. The two small arrows in **a** indicate that the recovery vs. time data had not plateaued, and hence the ultimate recovery is slightly higher than the symbols shown



with decreasing stress. The corresponding power law exponents (-0.1 and -0.08) are negative as already expected from a qualitative examination of Figs. 3b and 4c. To our knowledge, such behavior has not been noted in two-phase blends previously. Furthermore, for both these blends, the dependence of the recovery time on stress is characterized by exponents of -1.1 and -1.3 ; that is, λ_{F2} increases more steeply than σ^{-1} . These observations suggest that PTFE particles promote the coalescence of PDMS drops in PI, and Fe particles promote the coalescence of PI drops in PDMS.

S20-Fe The behavior of this sample is intermediate between the above two trends. As compared to the behavior of S20-0, the trend of $\gamma_\infty \propto \sigma^{0.11}$ is a significantly weaker dependence, and $\lambda_{F2} \propto \sigma^{-0.72}$ is a significantly stronger dependence. Taken together, these suggest that, with decreasing stress, the drop size R increases more sharply than for the particle-free blend, i.e., Fe particles also promote coalescence of PDMS drops in

PI, although coalescence promotion is not as strong as in S20-PTFE and S80-Fe.

In summary, the rheological data suggest that

- FeOOH particles do not affect the qualitative trends in coalescence behavior of either PDMS drops in PI or PI drops in PDMS. However, a quantitative evaluation of the ultimate recovery and recovery time suggests that these particles may produce a smaller drop size in both blends.
- Fe particles strongly promote coalescence of PI drops in PDMS but may weakly promote coalescence of PDMS drops in PI.
- PTFE particles strongly promote coalescence of PDMS drops in PI. PTFE particles do not affect the qualitative trends in coalescence behavior of PI drops in PDMS, but a quantitative evaluation of the ultimate recovery and recovery time suggests that PTFE particles reduce the drop size in S80 blends.

Fig. 7 Variation of **a** γ_∞ , and **b** λ_{F2} with stress for S80 blends

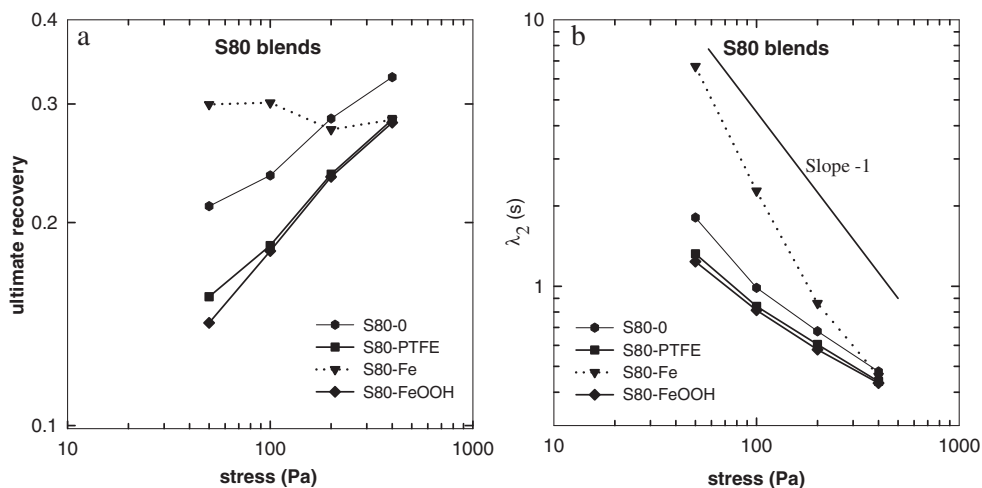


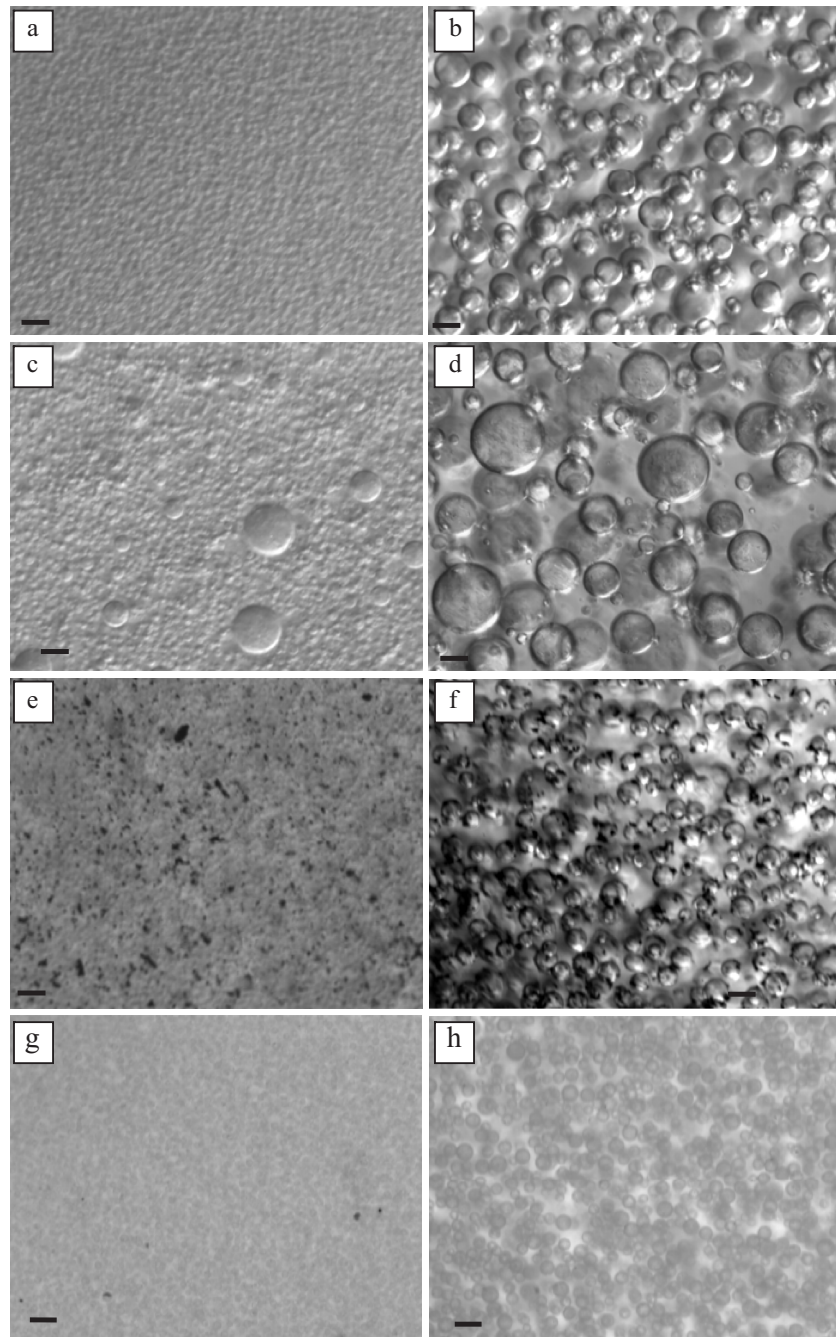
Table 3 Power law exponents for stress dependence of ultimate recovery and recovery time

Sample	Recovery exponent	Time exponent
S20-0	0.28	-0.56
S20-PTFE	-0.10	-1.10
S20-Fe	0.11	-0.72
S20-FeOOH	0.32	-0.53
S80-0	0.19	-0.63
S80-PTFE	0.27	-0.52
S80-Fe	-0.08	-1.30
S80-FeOOH	0.30	-0.50

Flow visualization

The goal of this section is to confirm the above rheology-derived conclusions by direct visualization. Due to intense scattering from the samples, flow visualization requires a significantly smaller gap than the rheology experiments. Accordingly, wall effects are more significant, and effect such as sedimentation may also become significant in long-duration experiments. The flow history of Fig. 2 takes a relatively long time, and

Fig. 8 **a** and **b** S20-0, **c** and **d** S20-PTFE, **e** and **f** S20-Fe, **g** and **h** S20-FeOOH. *Left column* of images were taken after preshearing at a high rate. *Right column* were taken after further shearing at a lower rate. See text for details. All *scale bars* are 40 μm

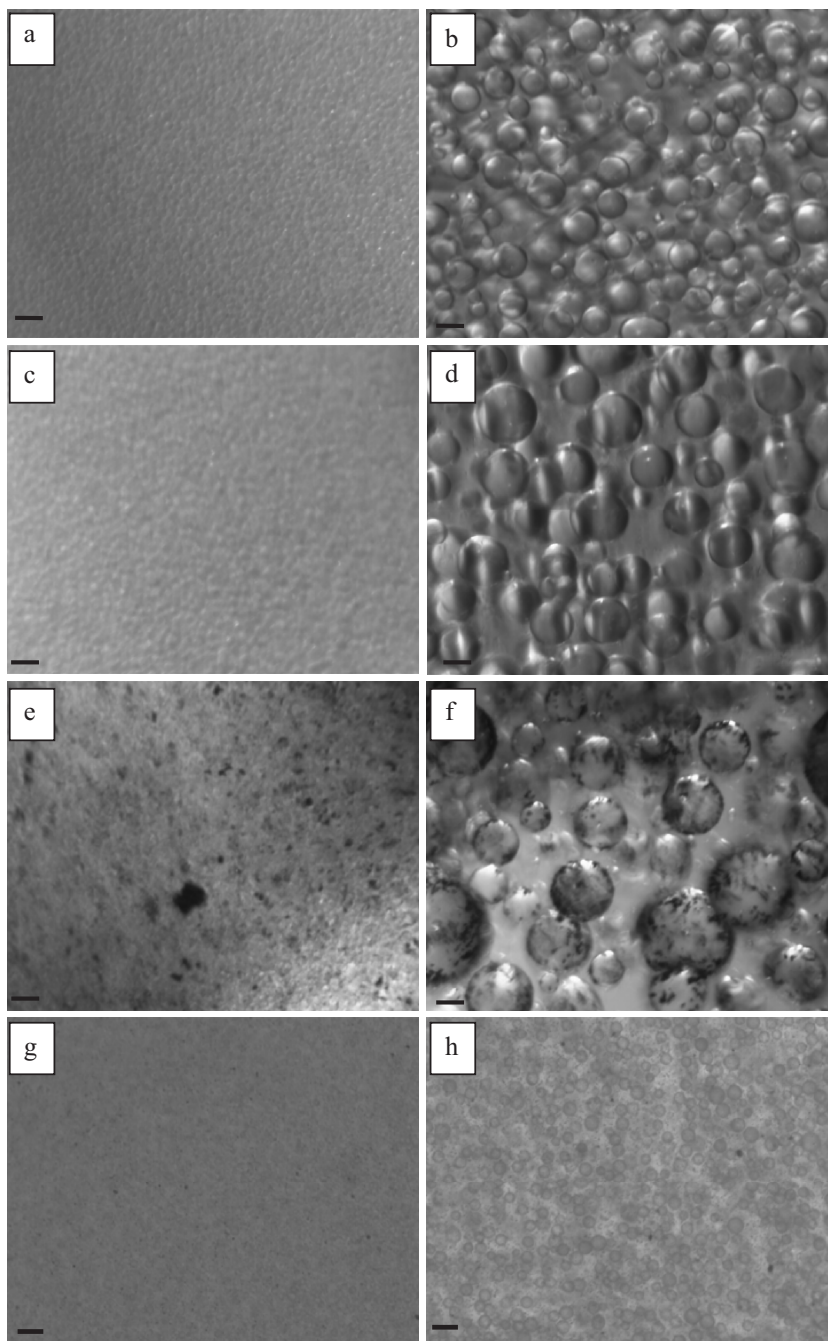


hence, a much simpler flow protocol was used for visualization studies. All the samples were first sheared at a high shear rate of 2.7 s^{-1} (which roughly corresponds to 400 Pa shear stress) for 2,000 strain units, and then, the shear rate was lowered to 0.29 s^{-1} (which roughly corresponds to a stress of 50 Pa) and the sample was sheared for an additional 3,000 strain units. This flow history is suitable for comparing the relative extents of flow-induced coalescence in the various samples.

The left column of Fig. 8 presents optical images of the four S20 blends after shearing at 2.7 s^{-1} for 3,000 strain units. While a two-phase structure is evident in all four images, in most cases, the drop sizes are too small to quantify from these images. The only exception is S20-PTFE, in which some large drops are already evident.

Upon stepping down the shear rate (right column of Fig. 8), flow-induced coalescence occurs in all cases;

Fig. 9 **a** and **b** S80-0, **c** and **d** S80-PTFE, **e** and **f** S80-Fe, **g** and **h** S80-FeOOH. *Left column* of images were taken after preshearing at a high rate. *Right column* were taken after further shearing at a lower rate. See text for details. All *scale bars* are $40 \mu\text{m}$



however, due to the larger size of drops, the differences between the various samples are clear. Specifically, S20-PTFE has significantly larger drops, and S20-FeOOH has significantly smaller drops than the corresponding particle-free blend. Significant differences between S20-Fe and S20-0 are not evident, at least from a simple inspection of the images. We also note in passing that the capillary number for the largest S20 drops at 0.29 s^{-1} are about 0.35, i.e., slightly lower than the value of about 0.5 expected for breakup of drops at this viscosity ratio.

Figure 9 shows the results of flow visualization for the S80 samples. Once again, after shearing at the high rate of 2.7 s^{-1} , the drop sizes are too small to be quantified. However, upon stepping down the rate to 0.29 s^{-1} , it is clear that S80-PTFE and S80-Fe both have significantly larger drops than S80-0, whereas S80-FeOOH has smaller drops than S80-0.

The flow visualization results generally support the conclusions drawn from the rheology study. Yet, the agreement is not perfect. The most notable discrepancy is that visualization clearly shows that drop size in S80-PTFE is larger than in S80-0. In direct contradiction, the S80-PTFE shows smaller values for γ_{∞} and λ_{F2} as compared to the S80-0 blend. The reasons for this discrepancy are not clear.

Discussion

We have shown that:

- Particles can both reduce the mean drop size as well as increase the mean drop size realized in a droplet/matrix blend.
- The effect on drop size can be symmetric (e.g., PTFE particles promote coalescence in both S20 and S80; FeOOH particles reduce drop size in both S20 and S80) or can be asymmetric (Fe particles promote coalescence in S80 but have no significant effect in S20).
- Particles can significantly affect the rheology, even qualitatively. For example, in S20-PTFE and in S80-Fe, the ultimate recovery increases with decreasing stress, a trend that is qualitatively different from that in the corresponding particle-free blend. Furthermore, the effect on rheology can be asymmetric as well; changing the continuous phase can sharply change the rheological behavior.
- Finally, while rheological behavior parallels trends in drop size in most cases, the correspondence is not perfect.

It must be emphasized that the above conclusions are based only on a few particles of certain sizes and types. Particles of other sizes or types may cause effects that are quite different, even qualitatively, from those observed here. For example, Fe particles of a much smaller size or at a much higher loading may be able to stop coalescence.

The first two items above warrant further comment. Extensive literature on oil–water emulsions suggests that interfacially adsorbed particles can stabilize Pickering emulsions (Binks 2002; Binks and Horozov 2006). Several mechanisms contribute to emulsion stability: steric hindrance of interfacially adsorbed particles hinders drop coalescence; a tightly packed interfacial monolayer of particles gives the drops a solid-like shell; in oil/water systems, charged particles at the interface induce electrostatic repulsion between drops. Thus, the decrease in drop size in polymer blends due to added particles, e.g., FeOOH, is not surprising; these blends may be regarded as polymeric analogs of oil/water Pickering emulsions. Indeed, the ability of interfacially adsorbed particles to decrease the phase size in polymer blends has been documented previously. (Elias et al. 2007; Hong et al. 2006; Si et al. 2006; Fenouillot et al. 2009).

The cases of increased drop size due to added particles, e.g., Fe particles in S80 blends, are more surprising and, to our knowledge, has not been documented in polymer blends previously. This phenomenon—particle-inducing coalescence—has been documented in oil–water emulsions, although the literature on this topic is relatively limited (Dickinson 2006; Kosaric et al. 1987; Mizrahi and Barnea 1970; Van Hamme et al. 2003). However, the related phenomenon of particles promoting coalescence of *bubbles* is very well-known, and in fact, highly hydrophobic particles are recognized as being effective defoaming agents for aqueous systems (Denkov and Marinova 2006; Garrett 1993; Pugh 1996). The generally accepted mechanism for such defoaming is “bridging–dewetting” as illustrated in Fig. 10. Consider a particle adsorbed on the surface of a bubble in water. If the particle is sufficiently hydrophobic (i.e., if the contact angle measured through the water phase exceeds 90°), only a small portion of the particle protrudes into the water phase (Fig. 10a). During a collision with another bubble, it is then possible to realize the situation of Fig. 10b, where the particle bridges across the thin water film separating the bubbles. Since the equilibrium contact angle exceeds 90° , the situation of Fig. 10b is unstable, and the contact line recedes across the interface until the film ruptures, inducing bubble coalescence. In effect, the bridged film ruptures because it dewets the hydrophobic particle.

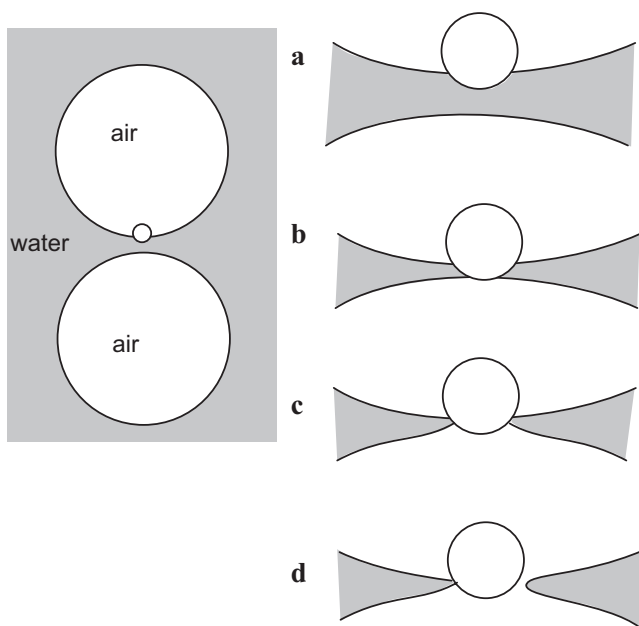


Fig. 10 Bridging–dewetting mechanism. *Left schematic* shows two gas bubbles colliding in water, where a hydrophobic particle is in the region between the bubbles. **a** Magnified view of hydrophobic particle adsorbed on one bubble. **b** Particle bridging across the film separating the two interfaces. **c** Lower contact line recedes across the hydrophobic particle. **d** Film ruptures

While the mechanism has been investigated primarily for foams, the principle is general: A particle that is preferentially wetted by the dispersed phase will promote coalescence of the dispersed phase. It is noteworthy that the above mechanism is inherently asymmetric: Bridging–dewetting–induced coalescence occurs only if the preferentially wetting phase is the drop phase. The reverse situation—the preferentially wetting phase being continuous—can give stable particle bridges across the drops and can stabilize drops against coalescence (Ashby et al. 2004; Horozov and Binks 2006; Stancik and Fuller 2004).

Certainly, the situation illustrated in Fig. 10b is overly simplistic. In particular, it has been noted that even particles that are preferentially wetted by water (have a contact angles slightly less than 90° when measured through the water phase) can be good defoaming agents. This has been attributed to their non-spherical shape and especially to sharp corners on particles, which can play a crucial role in bridging dewetting (Denkov and Marinova 2006; Garrett 1993; Pugh 1996).

We hypothesize that the coalescence promotion observed in this paper can be explained by the bridging–dewetting mechanism. Specifically, we hypothesize that Fe particles are preferentially wetted by PI; accordingly, they promote coalescence of PI drops in PDMS but do not promote coalescence of PDMS drops in PI.

In contrast, we hypothesize that the PTFE particles are preferentially wetted by the PDMS and hence strongly promote coalescence of PDMS drops in PI. Note that PTFE particles also weakly promote coalescence of PIS drops in PDMS, which may be attributable to their highly non-spherical shape.

Finally, it is important to note that this paper compares the different particle types at *fixed particle volume fraction*. The significant difference in the sizes of the different particle types implies a correspondingly large difference in the interfacial area that can be covered when the particles adsorb at an interface. In the case of FeOOH, tight interfacial coverage corresponds to roughly $2 \text{ m}^2/\text{g}$ of particles, i.e., $\sim 8 \times 10^6 \text{ m}^2/\text{m}^3$ of particles (Cheng and Velankar 2008, 2009). A simple geometric calculation (equating the surface area of the 20% drops to the area covered by 0.5% particles) suggests that, if all the FeOOH particles are at the interface, complete surface coverage of drops is achieved when the mean drop diameter reaches $30 \text{ }\mu\text{m}$. Figures 8h and 9h show that most drops are in this size range, i.e., if most FeOOH particles are at the interface, then these drops are nearly tightly covered with particles. For the other two particle types, the interfacial area corresponding to tight coverage has not been measured experimentally. Yet, this area can be readily estimated for the Fe particles since they are spherical; assuming a $3\text{-}\mu\text{m}$ particle size, we estimate an interfacial area of $0.5 \times 10^6 \text{ m}^2/\text{m}^3$ of particles at tight coverage. Thus, in order to be tightly covered with Fe particles, the drops would have to be $480 \text{ }\mu\text{m}$ in diameter; the capillary number of such drops under the applied flow would far exceed the capillary number for breakup. Since the actual drop size in Figs. 8f and 9f is much smaller, the surface coverage in the Fe-containing blends is far below that needed for tight packing. Since PTFE particles are not spherical, their interfacial area at tight packing is not as easy to estimate; nevertheless, it is also likely to be far smaller than of the FeOOH particles, and hence, the drops are also likely to be sparsely covered with PTFE particles. This difference in surface coverage may be a simple explanation for why the FeOOH particles are able to reduce drop size.

Summary

In summary, we have conducted experiments exploring the effects of interfacially active particles in droplet/matrix blends of immiscible homopolymers. We show that such interfacially adsorbed particles have a large effect on the morphology and rheology of blends of the homopolymers. Depending on the specific

particle type, particles can either increase or reduce the mean drop size in the blend. The changes in morphology can be tracked rheologically. Specifically, in creep-recovery experiments in increase (or decrease) in drop size due to added particles is generally reflected as an increase (or decrease) in the ultimate recovery and retardation time. Yet, the correspondence between drop size and recovery is not perfect, and it is clear that at least in some systems, the rheology is also affected by factors other than the drop size. That interfacially adsorbed particles can reduce mean drop size of a polymer blend was anticipated from the literature on Pickering emulsions. The reverse effect—an increase in drop size due to particles—may be an analog of the bridging–dewetting mechanism well-known from literature on foams.

Acknowledgements We thank Rhodia Silicones and Kuraray America for providing the PDMS and PI homopolymers, respectively. We are grateful to Elementis Inc., Dyneon Corp., and Prof. Phule (University of Pittsburgh) for making particles available for this research. This research was supported by a CAREER grant CBET- 0448845 from the National Science Foundation, USA.

References

- Ashby NP, Binks BP, Paunov VN (2004) Bridging interaction between a water drop stabilised by solid particles and a planar oil/water interface. *Chem Comm* (4): 436–437
- Binks BP (2002) Particles as surfactants—similarities and differences. *Curr Opin Colloid Interface Sci* 7:21–41
- Binks BP, Horozov TS (2006) Colloidal particles at liquid interfaces. Cambridge University Press, Cambridge
- Cheng HL, Velankar SS (2008) Film climbing of particle-laden interfaces. *Colloid Surf A* 315:275–284
- Cheng HL, Velankar SS (2009) Interfacial jamming of particle-laden interfaces studied in a spinning drop tensiometer. *Langmuir* 25:4412–4420
- Datta S, Lohse DJ (1996) Polymeric compatibilizers. Hanser, Munich
- Denkov ND, Marinova KG (2006) Antifoam effects of solid particles, oil drops, and oil-solid compounds in aqueous foams. In: Binks BP, Horozov TS (eds) Colloidal particles at liquid interfaces. Cambridge University Press, Cambridge
- Dickinson E (2006) Interfacial particles in food emulsions and foams. In: Binks BP, Horozov TS (eds) Colloidal particles at liquid interfaces. Cambridge University Press, Cambridge
- Elias L, Fenouillot F, Majeste JC, Cassagnau P (2007) Morphology and rheology of immiscible polymer blends filled with silica nanoparticles. *Polymer* 48:6029–6040
- Elias L, Fenouillot F, Majeste JC, Martin G, Cassagnau P (2008) Migration of nanosilica particles in polymer blends. *J Polym Sci Polym Phys* 46:1976–1983. doi:10.1002/polb.21534
- Fenouillot F, Cassagnau P, Majeste JC (2009) Uneven distribution of nanoparticles in immiscible fluids: Morphology development in polymer blends. *Polymer* 50:1333–1350. doi:10.1016/j.polymer.2008.12.029
- Garrett PR (1993) Mode of action of antifoams. In: Garrett PR (ed) Defoaming. Marcel Dekker, New York
- Graebbling D, Muller R, Palierne JF (1993) Linear viscoelastic behavior of some incompatible polymer blends in the melt. Interpretation of data with a model of emulsion of viscoelastic liquids. *Macromolecules* 26:320–329
- Gramespacher H, Meissner J (1995) Reversal of recovery direction during creep recovery of polymer blends. *J Rheol* 39:151–160
- Gubbels F, Jerome R, Teyssie P, Vanlathem E, Deltour R, Calderone A, Parente V, Bredas JL (1994) Selective localization of carbon-black in immiscible polymer blends—a useful tool to design electrical conductive composites. *Macromolecules* 27:1972–1974
- Hong JS, Namkung H, Ahn KH, Lee SJ, Kim C (2006) The role of organically modified layered silicate in the breakup and coalescence of droplets in PBT/PE blends. *Polymer* 47:3967–3975
- Horozov TS, Binks BP (2006) Particle-stabilized emulsions: a bilayer or a bridging monolayer? *Angew Chemie Int Ed* 45:773–776
- Kitade S, Ichikawa A, Imura N, Takahashi Y, Noda I (1997) Rheological properties and domain structures of immiscible polymer blends under steady and oscillatory shear flows. *J Rheol* 41:1039–1060
- Kosaric N, Cairns WL, Gray NCC (1987) Microbial deemulsifiers. In: Kosaric N, Cairns WL, Gray NCC (eds) Biosurfactants and biotechnology, vol 25. Marcel Dekker, New York, pp 247–321
- Macosko CW, Guegan P, Khandpur AK, Nakayama A, Marechal P, Inoue T (1996) Compatibilizers for melt blending: pre-made block copolymers. *Macromolecules* 29:5590–5598
- Martin JD (2007) The effect of surface-active block copolymers on two-phase flow. PhD thesis, Chemical Engineering, University of Pittsburgh, Pittsburgh
- Martin JD, Velankar SS (2007) Effects of compatibilizer on immiscible polymer blends near phase inversion. *J Rheol* 51:669–692
- Milner ST, Xi H (1996) How copolymers promote mixing of immiscible homopolymers. *J Rheol* 40:663–687
- Mizrahi J, Barnea E (1970) Effects of solid additives on the formation and separation of emulsions. *Br Chem Eng* 15:497–503
- Pugh RJ (1996) Foaming, foam films, antifoaming and defoaming. *Adv Colloid Interface Sci* 64:67–142
- Ray SS, Pouliot S, Bousmina M, Utracki LA (2004) Role of organically modified layered silicate as an active interfacial modifier in immiscible polystyrene/polypropylene blends. *Polymer* 45:8403–8413
- Si M, Araki T, Ade H, Kilcoyne ALD, Fisher R, Sokolov JC, Rafailovich MH (2006) Compatibilizing bulk polymer blends by using organoclays. *Macromolecules* 39:4793–4801
- Stancik EJ, Fuller GG (2004) Connect the drops: using solids as adhesives for liquids. *Langmuir* 20:4805–4808
- Sumita M, Sakata K, Asai S, Miyasaka K, Nakagawa H (1991) Dispersion of fillers and the electrical conductivity of polymer blends filled with carbon black. *Polymer Bull* 25:266–271
- Thareja P (2008) Study of particles at fluid/fluid interfaces. PhD Thesis, Chemical Engineering, University of Pittsburgh, Pittsburgh
- Thareja P, Velankar SS (2007) Particle-induced bridging in immiscible polymer blends. *Rheol Acta* 46:405–412
- Thareja P, Velankar S (2008a) Rheology of immiscible blends with particle-induced drop clusters. *Rheol Acta* 47:189–200

- Thareja P, Velankar SS (2008b) Interfacial activity of particles at PI/PDMS and PI/PIB interfaces: analysis based on Girifalco-Good theory. *Colloid Polym Sci* 286:1257–1264
- Tucker CL, Moldenaers P (2002) Microstructural evolution in polymer blends. *Ann Rev Fluid Mech* 34:177–210
- Van Hamme JD, Singh A, Ward OP (2003) Recent advances in petroleum microbiology. *Microbiol Mol Biol Rev* 67:503–549
- Van Puyvelde P, Velankar S, Moldenaers P (2001) Rheology and morphology of compatibilized polymer blends. *Curr Opin Colloid Interface Sci* 6:457–463
- Vermant J, Cioccolo G, Nair KG, Moldenaers P (2004) Coalescence suppression in model immiscible polymer blends by nano-sized colloidal particles. *Rheol Acta* 43:529–538
- Vinckier I, Mewis J, Moldenaers P (1996) Relationship between rheology and morphology of model blends in steady shear flow. *J Rheol* 40:613–632
- Vinckier I, Moldenaers P, Mewis J (1999) Elastic recovery of immiscible blends 1. Analysis after steady state shear flow. *Rheol Acta* 38:65–72
- Wang J, Velankar S (2006a) Strain recovery of model immiscible blends without compatibilizer. *Rheol Acta* 45:297–304
- Wang J, Velankar S (2006b) Strain recovery of model immiscible blends: effects of added compatibilizer. *Rheol Acta* 45:741–753
- Zaikin AE, Zharinova EA, Bikmullin RS (2007) Specifics of localization of carbon black at the interface between polymeric phases. *Polym Sci, Ser A* 49:328–336